0090-9556/10/3804-655–666$20.00
DRUG METABOLISM AND DISPOSITION
Vol. 38, No. 4
30239/3568964
DMD 38:655–666, 2010
Printed in U.S.A.

Disposition of [1′-^{14}C]Stavudine after Oral Administration to Humans

Lian Zhou, Sanjeev Kaul, Peggy Liu-Kreyche, Scott B. Tran, Robert R. Espina,[1] Bethanne M. Warrack, Vikram A. Roongta, and Ramaswamy A. Iyer

Department of Biotransformation (L.Z., P.L.-K., R.A.I.), Discovery Medicine and Clinical Pharmacology (S.K.), Chemical Synthesis (S.B.T.), and Discovery Analytical Sciences (R.R.E., B.M.W., V.A.R.), Bristol-Myers Squibb Co., Princeton, New Jersey

Received September 14, 2009; accepted January 6, 2010

ABSTRACT:

The disposition of stavudine, a potent and orally active nucleoside reverse transcriptase inhibitor, was investigated in six healthy human subjects. Before dosing humans with [1′-^{14}C]stavudine, a tissue distribution study was performed in Long-Evans rats. Results from this study showed no accumulation of radioactivity in any of the tissues studied, indicating that the position of the ^{14}C-label on the molecule was appropriate for the human study. After a single 80-mg (100 μCi) oral dose of [1′-^{14}C]stavudine, approximately 95% of the radioactive dose was excreted in urine with an elimination half-life of 2.35 h. Fecal excretion was limited, accounting for only 3% of the dose. Unchanged stavudine was the major drug-related component in plasma (61% of area under the plasma concentration-time curve from time zero extrapolated to infinite time of the total plasma radioactivity) and urine (67% of dose). The remaining radioactivity was associated with minor metabolites, including mono- and bis-oxidized stavudine, glucuronide conjugates of stavudine and its oxidized metabolite, and an *N*-acetylcysteine (NAC) conjugate of the ribose (M4) after glycosidic cleavage. Formation of metabolite M4 was shown in human liver microsomes incubated with 2′,3′-didehydrodideoxyribose, the sugar base of stavudine, in the presence of NAC. In addition, after similar microsomal incubations fortified with GSH, two GSH conjugates, 3′-GS-deoxyribose and 1′-keto-2′,3′-dideoxy-3′-GS-ribose, were observed. This suggests that 2′,3′-didehydrodideoxyribose underwent cytochrome P450-mediated oxidation leading to an epoxide intermediate, 2′,3′-ribose epoxide, followed by GSH addition. In conclusion, absorption and elimination of stavudine were rapid and complete after oral dosing, with urinary excretion of unchanged drug as the predominant route of elimination in humans.

Stavudine (also known as 2′,3′-didehydro-3′-deoxythymidine, Zerit, and d4T), a synthetic thymidine nucleoside analog, is a potent, selective, and orally active antiretroviral agent. Since its introduction to the market in 1994, stavudine has been widely used in combination antiretroviral therapy for the treatment of HIV infections in adults and children (Lea and Faulds, 1996; Siegfried et al., 2006). The mechanism of action of stavudine involves sequential phosphorylation by cellular kinases to its active metabolite, stavudine-5′-triphosphate, which inhibits the HIV-1 reverse transcriptase enzyme, and causes DNA chain termination by incorporating into viral DNA (Huang et al., 1992).

A number of in vitro and in vivo studies have been conducted with ^{14}C-labeled stavudine to understand its disposition and metabolic fate. In vitro biotransformation studies with stavudine in rat hepatocytes and monkey liver S9 fractions revealed that the majority of stavudine remained unchanged with limited stavudine converted to thymine. When stavudine was incubated with human liver slices for 6 h, 87% of radioactivity was accounted for by unchanged drug; 2% was metabolized to thymine; and 7% was associated with unidentified polar compounds (Kaul et al., 1999). These data suggested that stavudine was not metabolized extensively. Disposition studies in mice, rats, and monkeys dosed orally with [2-^{14}C]stavudine, [4-^{14}C]stavudine, or [5-^{3}H]stavudine (all labels on the thymidine moiety) showed that the compound was well absorbed (Russell et al., 1990; Cretton et al., 1993; Kaul and Dandekar, 1993; Kaul et al., 1999). The recovery of the drug in excreta varied in animals, with the majority of the dose recovered in the urine. Fecal excretion was minimal, averaging <1.5% of the dose in the animal studies. Furthermore, in rats approximately 14% of the dose was recovered as $^{14}CO_2$ in expired air (Kaul et al., 1999). In all three species—mice, rats, and monkeys—the majority of the radioactivity in plasma, urine, and feces was represented by unchanged drug, consistent with the in vitro observation of relatively slow biotransformation of stavudine. Because the dose recovery in excreta was low in monkeys (40% in urine, <1.5% in feces), it has been suggested that a considerable portion of stavudine could be metabolized and retained in monkeys. This was based on the fact that thymine and its metabolite, β-aminoisobutyric

[1] Current affiliation: Wyeth Research, Collegeville, PA.

Article, publication date, and citation information can be found at http://dmd.aspetjournals.org.
doi:10.1124/dmd.109.030239.

ABBREVIATIONS: ADME, absorption, distribution, metabolism, and elimination; CPM, counts per minute; TD, tissue distribution; NAC, *N*-acetyl-L-cysteine; LC/MS, liquid chromatography/mass spectrometry; TRA, total radioactivity; LSC, liquid scintillation counting; LLOQ, lower limit of quantitation; MS/MS, tandem mass spectrometry; QC, quality control; AUC(INF), area under the plasma concentration-time curve from time zero extrapolated to infinite time; HPLC, high-performance liquid chromatography; TOCSY, total correlation spectroscopy.

acid, were detected in the plasma and urine of monkeys, and thymine could have been incorporated into endogenous molecules through pathways of purine and pyrimidine metabolism (Cretton et al., 1993). Both the recovery of dose in expired air of rats and the poor recovery in the monkeys suggested that labeling the thymine ring was not ideal for further absorption, distribution, metabolism, and elimination (ADME) studies.

The total fate of stavudine, including mass balance, routes of excretion, metabolic pathways, and exposure to stavudine-related material in circulation, has not been completely established in humans. The present study investigated the pharmacokinetics and disposition of [1′-^{14}C]stavudine after a single 80-mg (100 μCi) oral dose to six healthy human subjects. The decision to label the ribose ring instead of the thymine ring was based on the animal data described above where loss of label was observed. Before conducting the human ADME study, a tissue distribution (TD) study in Long-Evans rats was conducted with [1′-^{14}C]stavudine to ensure the projected radiation exposure in humans after a 100-μCi oral dose is below the safety exposure limit (International Commission on Radiological Protection, 2008). As part of the rat study, expired air was collected to confirm the metabolic stability of the label. Here we present data from both the TD study in rats and the human ADME study. Also presented are metabolites that arise from metabolism of the ribose ring that could be easily followed because of the label on the ribose ring.

Materials and Methods

Chemicals and Biologicals. Stavudine and its internal standard, d4-stavudine (6-[D]-1-(5-(hydroxymethyl)-2,5-dihydrofuran-2-yl)-5-[CD_3]methylpyrimidine-2,4(1*H*,3*H*)-dione), were synthesized chemically at Bristol-Myers Squibb Research and Development (Princeton, NJ). [1-^{14}C]D-Ribose (51 mCi/mmol, packaged in water/MeOH, 5:1, at concentration of 16.7 mCi/ml and radiochemical purity >97%) was purchased from ViTrax (Placentia, CA). Formic acid and ammonium acetate were purchased from Mallinckrodt Baker, Inc. (Phillipsburg, NJ). NADPH, GSH, and *N*-acetyl-L-cysteine (NAC) were purchased from Sigma-Aldrich (St. Louis, MO). Carbo-Sorb E $^{14}CO_2$ trapping solution, Hionic Fluor, and Permafluor E$^+$ liquid scintillation mixture were obtained from PerkinElmer Life and Analytical Sciences (Waltham, MA). Ecolite liquid scintillation mixture was purchased from MP Biomedicals (Solon, OH). Deionized water was prepared with a Milli-Q plus ultrapure water system (Millipore Corporation). Pooled human liver microsomes were purchased from BD Gentest (Woburn, MA). All the other chemicals used were reagent grade or better.

Synthesis of [1′-^{14}C]Stavudine. [1′-^{14}C]Stavudine was synthesized from its ^{14}C-labeled precursor [1-^{14}C]D-ribose based on a synthetic procedure reported by Discordia (1996). The synthesis of [1′-^{14}C]stavudine was accomplished in 10 chemical steps in a total yield of 20.5% with specific activity of 15.53 μCi/mg, chemical purity of 99.3%, and radiochemical purity of 99.6%.

Acidic Hydrolysis of [1′-^{14}C]Stavudine. Hydrochloric acid solution (9% w/w) was prepared by mixing 1 volume of hydrochloric acid (approximately 36% w/w) with 3 volumes of water. Portions (1 ml each) of [1′-^{14}C]stavudine methanol stock (15.6 μCi/ml) were transferred to a 5-ml glass tube and dried under a stream of N_2 gas. Hydrolysis reactions were started by adding 1 ml of 9% hydrochloric acid into glass tubes. The glass tubes were kept in a shaking water bath at 90°C for 2 h. The reaction mixtures were evaporated to dryness on a Savant SpeedVac SPD2010 Concentrator (Thermo Fisher Scientific, Waltham, MA) at room temperature. The residue was suspended in 100 μl of 100 mM phosphate buffer, pH 7.4, and kept at −20°C until incubated with human liver microsomes. The reaction was monitored by liquid chromatography/mass spectrometry (LC/MS) and LC/radioactivity detection. Approximately 70% of [1′-^{14}C]stavudine was hydrolyzed to [1′-^{14}C]2′,3′-didehydrodideoxyribose after 2-h incubation. No further purification steps were performed on the final reaction mixtures. [1′-^{14}C]2′,3′-Didehydrodideoxyribose coexisted with its byproduct thymine and its precursor [1′-^{14}C]stavudine.

Incubation with Human Liver Microsomes. Human liver microsomes were incubated with a substrate mixture of [1′-^{14}C]stavudine, [1′-^{14}C]2′,3′-didehydrodideoxyribose, and thymine, in presence or absence of either GSH or NAC. The substrate mixture was generated as described above. The concentration of 2′,3′-didehydrodideoxyribose used in the microsomal incubation was approximate 40 μM. The concentrations of microsomal proteins, NADPH, and phosphate buffer were 1 mg/ml, 1 mM, and 100 mM, respectively. For incubation performed in the presence of either GSH or NAC, the concentrations of both the reagents used were 5 mM. The reaction was initiated by addition of NADPH to the incubation mixture. The incubations were carried out in microcentrifuge tubes at 37°C for 30 min in a shaking water bath at a final volume of 200 μl. Incubations were stopped by cooling on ice after addition of 200 μl of acetonitrile. The incubation mixture was then centrifuged at 14,000 rpm for 2 min in an Eppendorf model 5417C centrifuge (Eppendorf AG, Hamburg, Germany). The supernatants were removed and evaporated to near dryness under a stream of nitrogen. The residues were reconstituted in 50 μl of water and kept at −20°C until analysis. Incubations with [1′-^{14}C]stavudine (40 μM) or with thymine (40 μM) were performed in parallel. Incubation in the absence of the microsomal protein and incubation in absence of the cofactor NADPH were used as negative controls.

TD Study in Rats and Sample Preparation. Experiments were performed according to the *Guide for the Care and Use of Laboratory Animals* (Institute of Laboratory Animal Resources, 1996). The study consisted of eight groups of three male Long-Evans rats. [1′-^{14}C]Stavudine in deionized water was administered at a target dose level of 5 mg/kg (100 μCi/kg) as a single oral gavage dose to overnight-fasted animals. The animals in group 1 did not receive test article and were euthanized to provide control samples. The remaining animals were euthanized at 1 h (group 2), 4 h (group 3), 12 h (group 4), 24 h (group 5), 48 h (group 6), 96 h (group 7), and 168 h (group 8) after dosing. Animals in group 6 were placed in glass metabolism cages, and their expired ^{14}CO2 was trapped in potassium hydroxide solution (6 M) and collected at 0 to 6, 6 to 12, 12 to 24, and 24 to 48 h postdose. Blood samples were collected just before euthanasia. A portion of blood samples was centrifuged for 10 min at 1000*g* and 5°C for plasma. After euthanasia of the animals, 21 major tissues and gastrointestinal contents were excised from each animal.

Disposition Study in Humans and Sample Preparation. This was an open-label single-dose study. An 8-ml oral solution of [1′-^{14}C]stavudine (80 mg, 100 μCi) was administered to six healthy male subjects. An 80-mg dose represents the total daily dose used in clinical practice for the treatment of HIV infection. Blood samples were collected for analysis of stavudine and total radioactivity (TRA) determinations at 0, 0.5, 1, 1.5, 2, 4, 6, 8, 12, 24, 36, and 48 h and every 24 h for the subsequent study period (0–168 h). Additional blood samples at 1, 2, 6, 12, 24, and 48 h were collected for biotransformation studies. Plasma was prepared from the blood samples by centrifuging for 10 min at 1000*g* and 5°C. Urine was collected at 6-h intervals for the first day and over 24-h intervals until end of the study period (0–168 h) for analysis of stavudine, TRA determination, and biotransformation studies. Feces were collected at 24-h intervals over the 168-h study period for TRA determination and biotransformation studies.

Pooled plasma, urine, and fecal samples were prepared for biotransformation studies. Plasma samples at 1, 2, 4, and 6 h were pooled by combining equal volumes of individual plasma samples at a given time point. Pooled urine and fecal samples were prepared by combining 1% by weight of urine and fecal homogenates excreted during each collection interval from all six subjects over 168 h postdose.

Liquid Scintillation Counting for TRA Determination. Radioactivity in samples obtained from the rat TD study and the human disposition study was determined with a Model LS 6500 liquid scintillation counter (Beckman Coulter, Inc., Fullerton, CA) or a Tri-Carb 3100TR liquid scintillation analyzer (PerkinElmer Life and Analytical Sciences). Before radioanalysis, tissue samples, gastrointestinal content samples, and fecal samples were homogenized with water to form a 20% (w/w) homogenate using a PT 45-80 probe homogenizer (Kinematica Polytron; Kinematica, Littau-Lucerne, Switzerland). Aliquots of blood (approximately 0.05 g), homogenized tissue (0.02–0.05 g), gastrointestinal content (0.2–0.3 g), and homogenized fecal (0.2–0.3 g) samples were placed in cones and pads, dried, and combusted. The combustions were performed using a model 307 or model 387 Sample Oxidizer (PerkinElmer Life and Analytical Sciences). The resulting $^{14}CO_2$ was trapped in Carbo-Sorb E (PerkinElmer Life and Analytical Sciences). After the $^{14}CO_2$ trapping, Permafluor E$^+$ scintillation mixture (PerkinElmer Life and Analytical Sciences) was added, and the mixture was analyzed. Each small organ

(adrenal glands, eyes, thyroids, and urinary bladders) that was not homogenized was dried and combusted as a single sample. Aliquots (0.08–0.1 g) of potassium hydroxide solution with trapped expired $^{14}CO_2$ were mixed with deionized water (1 ml) and Hionic Fluor liquid scintillation mixture (5.5 ml; (PerkinElmer Life and Analytical Sciences) before liquid scintillation counting (LSC) analysis for TRA. Aliquots (0.1 g) of individual plasma samples and aliquots (0.2–0.3 g) of individual urine samples were mixed with Emulsifier-Safe scintillation fluid (PerkinElmer Life and Analytical Sciences) and analyzed by LSC.

All the samples were counted for 10 min or the time to reach 5% 2-ó error. LSC data were automatically corrected for counting efficiency using an external standardization technique and an instrument-stored quench curve generated from a series of sealed quench standards and reported as disintegrations per minute. The lower limit of quantitation (LLOQ) of radioactivity, based on a specific activity of 1.25 μCi/mg [1′-^{14}C]stavudine and detection background of 33.74 disintegrations per minute, was 120 ng-Eq of stavudine per gram of sample. The TRA was converted from ng-Eq/g to ng-Eq/ml for plasma and urine samples by considering specific gravity of both biological matrices to be 1. The TRA in feces was expressed in ng-Eq/g unit.

Assays of Stavudine in Plasma and Urine of Humans. Plasma and urine samples from human disposition studies were analyzed for unchanged stavudine by validated LC/tandem MS (MS/MS) methods. The internal standard used for both assays was d4-stavudine. The samples were prepared by a solid-phase extraction using 3M Empore C18 96-well solid-phase extraction plates (Varian, Inc., Palo Alto, CA). The plates were conditioned sequentially with 100 μl of methanol and 200 μl of water. After loaded with 450 μl of the sample/internal standard mixture, the plate was washed with 250 μl of water, and the elution was done with 75 μl of 0.1% formic acid in methanol. The eluant was directly analyzed by LC/MS/MS. Chromatographic separation was performed on a Shimadzu (Kyoto, Japan) Class VP system equipped with a system controller (model SCL-10A), two pumps (model LC-10AD), and an autoinjector (model SIL-10AD). A Metasil basic dC18 column (2 × 50 mm, 5 μm; Metachem Technologies, Inc., Torrance, CA) was used with the solvent system consisting of solvent A, 0.1% formic acid in water, and solvent B, methanol. A gradient was used where solvent A was held at 90% for 0.3 min and then decreased to 30% in the next 1.7 min before re-equilibrium. A Sciex API 3000 (Applied Biosystems/MDS Sciex, Foster City, CA) was used for plasma analysis, and an API 365 was used for urine analysis. Multiple reaction monitoring mode under optimized conditions was used for detection of stavudine and internal standard d4-stavudine. The transition m/z 225→m/z 127 was used for stavudine detection and m/z 229→m/z 131 for d4-stavudine detection. The standard curve ranges for the plasma and urine assay were 0.500 to 1000 μg/ml and 5.00 to 1000 μg/ml, respectively. Spiked analytical quality control (QC) samples were analyzed along with the study samples for assessment of the accuracy and precision of each analytical run. The QC samples at low, medium, and high concentration range of the standard curve were included in the analytical run in a minimum of two replicates. Deviations from the predicted concentrations for at least two thirds of the QC samples were within ±15% of their nominal values at all the concentration levels, with at least one QC sample at each level meeting the acceptance criteria. The LLOQs of the assay were 0.500 ng/ml in plasma and 5.00 ng/ml in urine.

Pharmacokinetic Analysis. In each sample of rats, the concentration of TRA was expressed as stavudine-equivalents. Blood, plasma, and tissue radioactivity concentration-time data were subjected to noncompartmental pharmacokinetic analysis.

Plasma concentration versus time data for stavudine and TRA from human disposition study were analyzed by a noncompartmental method using Kinetica 4.2 within the eToobox (version 2.2) (Thermo Fisher Scientific). The peak concentration (C_{max}) and the time to peak concentration (T_{max}) were obtained from experimental observations. The terminal log-linear phase of the concentration-time curve was identified by least-squares linear regression of at least three data points that yield a maximum G-criterion. The half-life of the terminal log-linear phase was calculated as Ln2/k, where k is the absolute value of the slope of the terminal log-linear phase. The area under the concentration-time curve, AUC(INF), was determined by using the mixed log-linear trapezoidal method. Oral clearance was calculated as the quotient of dose and AUC(INF). Renal clearance was estimated by dividing total urinary recovery (0-T) by AUC(0-T), where T was the same for both matrices. The binding of stavudine to serum proteins was minor (<10%) (Kaul et al., 1999); therefore, the renal clearance was not corrected for plasma protein binding.

Extraction of Human Plasma, Urine, and Fecal Samples for Biotransformation Analysis. *Plasma.* A 2-ml aliquot of pooled plasma sample was extracted by sequentially adding 2 volumes of methanol/acetonitrile (1:1 v/v) and 120 μl of 50% trichloroacetic acid. After addition of organic solvent, samples were vortexed to resuspend the solid material and then sonicated for 5 min. The extracted samples were centrifuged at 3000 rpm for 60 min at 5°C in an Eppendorf model 5810R centrifuge, and the supernatant was removed and saved. The residue was re-extracted two more times as described above. The combined supernatants were evaporated to dryness at room temperature under a stream of nitrogen gas. The dried residue was reconstituted in methanol/water (1:1 v/v). The samples were then centrifuged at 14,000 rpm for 2 min in an Eppendorf model 5417C centrifuge. Aliquots of the supernatants were injected onto the high-performance liquid chromatography (HPLC) system for biotransformation profiling or analyzed by LSC for radioactivity recovery. The extraction recovery of radioactivity ranged from 74 to 85%.

Urine. A 2-ml portion of the 0- to 168-h pooled urine was evaporated to dryness at room temperature under a stream of nitrogen. The dried residue was reconstituted in 100 μl methanol/water (1:1 v/v). The sample was then centrifuged at 14,000 rpm for 2 min in an Eppendorf model 5417C centrifuge. An aliquot of the supernatants was injected onto the HPLC system for biotransformation profiling. The pooled 0- to 24-h urine sample from subject 5 was used for isolation of metabolite M4. It was prepared by combining 50 ml of urine collected at 6, 12, and 24 h from subject 5. The sample was extracted by addition of 2 volumes of acetone/acetonitrile (1:1 v/v). After addition of organic solvent, the sample was vortexed, sonicated, and centrifuged at 3000 rpm for 10 min. The supernatant was transferred and evaporated to dryness on a Savant SpeedVac SPD2010 Concentrator at room temperature. The residue was reconstituted in 10 ml of 10% acetonitrile in water and centrifuged at 14,000 rpm for 2 min. The supernatant was injected onto a preparative HPLC system (Class VP; Shimadzu) for metabolite isolation.

Feces. A 1-g portion of the 0- to 168-h pooled fecal homogenate was extracted by addition of 2 ml of acetonitrile. The mixture was then vortexed, sonicated, and centrifuged at 3000 rpm for 10 min. The supernatants were removed and saved. The pellet was then extracted two more times with 2 ml of acetonitrile/water (3:1, v/v). The supernatants were combined and evaporated to dryness on a Savant SpeedVac SPD2010 Concentrator. The residue was reconstituted in methanol/water (1:1 v/v). An aliquot of the supernatant was injected onto an HPLC for biotransformation profiling or analyzed by LSC for radioactivity recovery. The extraction recovery of radioactivity was 91.5%.

HPLC for Biotransformation Analysis. Three HPLC methods were developed for the following purposes: method 1 for biotransformation profiling, method 2 for metabolite M4 isolation, and method 3 for sample analysis from acidic hydrolysis of [1′-^{14}C]stavudine and from microsomal incubations. Biotransformation profiling of pooled plasma (1, 2, 4, and 6 h), urine (0–168 h), and fecal (0–168 h) samples was done by HPLC method 1. It was performed on a Shimadzu Class VP system equipped with a system controller (model SCL-10A), two pumps (model LC-10AD), an autoinjector (model SIL-10AD), and a photodiode array detector (model SPD-M10A). A Waters (Milford, MA) Atlantis dC18 column (3.9 × 150 mm, 3 μm) was used with the solvent system consisting of solvent A, 10 mM ammonium acetate buffer, pH 6.5, and solvent B, a mixture of 200 ml of solvent A, 500 ml of acetonitrile, and 300 ml of methanol. A gradient was used where solvent A was held at 100% for 15 min and then decreased to 75% in the next 25 min. Preparative HPLC isolation of M4 from the pooled urine sample was performed by HPLC method 2. It used a Shimadzu Class VP system equipped with a system controller (model SCL-10A), two pumps (model LC-8A), an autoinjector (model SIL-10AP), a fraction collector (model FRC-10A), and an IN/US Systems (Tampa, FL) radioactivity detector (β-ram model 3). A Waters/YMC Europe GmbH (Dinslaken, Germany) C18 column (20 × 100 mm, 3 μm) was used for separation of drug-related components. The solvent system used was the same as in HPLC method 1. A two-step linear gradient was formed as follows: 0 min, 0% B; 30 min, 20% B; 31 min, 100% B; and 32 min, 100% B. The column was re-equilibrated at 0% B for 5 min before the next injection. Fractions of column eluant collected at 18.5 min (M4) were evaporated to dryness on a Savant SpeedVac SPD2010 Concentrator for further LC/MS/MS, accurate mass, and NMR analysis. The samples from acidic hydrolysis of [1′-^{14}C]stavudine and

from microsomal incubations were analyzed by HPLC method 3, in which an Agilent 1100 HPLC system (Agilent Technologies, Santa Clara, CA) was used. The mobile phases consisted of (A) water with 0.1% formic acid and (B) acetonitrile with 0.1% formic acid. The gradient and column used were the same as in HPLC method 1. HPLC method 3 used mobile phases containing no ammonium-related solvent modifiers to avoid observation of ammoniated adducts in the mass spectra. All the HPLC methods had a column temperature at 40ºC. HPLC methods 1 and 3 used a flow rate of 0.5 ml/min, whereas the HPLC method 2 had a flow rate of 10 ml/min.

Radioactivity Profiling of Human Plasma, Urine, and Feces. For radioactivity profiling of pooled human plasma, urine, and fecal samples, the HPLC eluant was collected in 0.25-min intervals on 96-well plates (Deepwell LumaPlate; PerkinElmer Life and Analytical Sciences) with a Gilson, Inc. (Middleton, WI) model FC 204 fraction collector. Each fraction of column eluate was evaporated to dryness on a Savant Speed-Vac and counted for radioactivity with a Packard Top Count microplate scintillation analyzer (PerkinElmer Life and Analytical Sciences). For each radiochromatographic profile, the average counts per minute (CPM) value of several early wells, in the range of 2 to 4 CPM, were designated as background (collected during elution of the void volume) and subtracted from the CPM value of each subsequent fraction. Profiles were prepared by plotting the resulting net CPM values against time after injection (Zhu et al., 2005). Radioactive peaks in the chromatographic profiles were reported as a percentage of the total radioactivity (CPM) recovered during the HPLC run.

LC/MS/MS. Mass spectrometric analyses of samples of pooled human plasma, urine, and feces and microsomal incubations were performed on a linear ion trap mass spectrometer (Thermo Fisher Scientific) equipped with an electrospray ionization probe operating in the positive ion mode. Samples were introduced into the mass spectrometer under the same HPLC conditions used for biotransformation profiling described above. For mass spectral analysis, half the eluant from the HPLC was directed into the mass spectrometer through a postcolumn splitter. The capillary temperature, nitrogen gas flow, spray current, and voltages were adjusted as needed to provide maximum sensitivity.

Accurate MS Analysis. Metabolite M4 isolated from pooled 0- to 24-h human urine of subject 5 was analyzed using a linear ion trap-FT hybrid linear ion trap Fourier transform ion cyclotron resonance mass spectrometer (Thermo Fisher Scientific) equipped with a NanoMate HD source (Advion BioSciences, Ithaca, NY) operated in positive ion mode. Accurate mass and MS/MS spectra were acquired by delivering approximately 100 ng/ml M4 in 1:1 water/acetonitrile containing 10 mM ammonium acetate at a flow rate of 150 nl/min. The resolving power of the Fourier transform ion cyclotron resonance mass analyzer was set at 12,500. Collision energy was set at 35%. The mass accuracy for all the ions observed was within 1.7 ppm of theory.

NMR. NMR analysis was performed on metabolite M4 isolated from pooled 0- to 24-h human urine of subject 5. NMR experiments were performed on a Bruker (Newark, DE) DRX 600-MHz NMR spectrometer equipped with an indirect detection 5-mm TXI Bruker Cryo-probe maintained at 30°C. The sample was dissolved in 200 μl of deuterium-labeled dimethyl sulfoxide. Chemical shifts were recorded in δ values (ppm) relative to tetramethylsilane. The WATERGATE (WATER suppression by GrAdient Tailored Excitation) solvent suppression scheme was applied during data acquisition to remove residual solvent signals. In total correlation spectroscopy (TOCSY), 8000 points were collected in t2 (24 transients per increment), and 480 points were collected in t1. Data were processed with zero filling to 8000 points in F2 and 2000 points in F1. Gaussian and sine bell square apodization functions were applied in both F1 and F2.

Results

TD Study in Rats. Mean radioactivity concentration (μg-Eq of stavudine/g) data for tissues and gastrointestinal contents are listed in Table 1. [1′-^{14}C]Stavudine was widely distributed in the tissues of rats after oral administration of a 5-mg/kg dose. T_{max} for all the tissues occurred at 1 h. T_{last} for tissues ranged from 4 h (skeletal muscle) to 168 h (heart, kidney, liver, and spleen). C_{max} values for tissues ranged from a high of 78.1 μg-Eq/g for urinary bladder to a low of 0.280 μg-Eq/g for brain. The next highest C_{max} values were for small intestine, kidneys, and stomach (8.40, 6.14, and 5.54 μg-Eq/g, respectively).

Mean tissue/plasma ratios of stavudine-equivalent concentrations of radioactivity at specified times through 48 h are listed in Table 2. The data are presented only through 48 h because that was the last

TABLE 1

Mean concentrations of radioactivity in tissues and gastrointestinal contents after a single oral (5 mg/kg) administration of [1′-^{14}C]stavudine to male rats

Matrix	Concentration[a]													
	Mean	S.D.	Mean	S.D.	Mean	S.D.	Mean	S.D.	Mean	S.D.	Mean	S.D.	Mean	S.D.
	1 h		*4 h*		*12 h*		*24 h*		*48 h*		*96 h*		*168 h*	
Adrenal glands	1.53	0.52	0.75	1.12	0.06	0.01	0.04	0.00	0.02	0.00	0.01	0.01	0.00	0.00
Blood	1.64	0.11	0.10	0.04	0.05	0.00	0.03	0.01	0.01	0.02	0.00	0.00	0.00	0.00
Bone (femur)	0.41	0.06	0.07	0.05	0.00	0.00	0.00	0.00	0.00	0.00	0.00	0.00	0.00	0.00
Bone marrow (femur)	1.75	0.08	0.15	0.07	0.05	0.04	0.00	0.00	0.00	0.00	0.00	0.00	0.00	0.00
Brain	0.28	0.01	0.09	0.02	0.02	0.00	0.01	0.00	0.00	0.00	0.00	0.00	0.00	0.00
Cecum	1.03	0.09	0.61	0.22	0.12	0.05	0.03	0.01	0.01	0.00	0.00	0.00	0.00	0.00
Cecum contents	0.06	0.03	0.49	0.14	0.05	0.04	0.01	0.01	0.00	0.00	0.00	0.00	0.00	0.00
Eyes	1.10	0.12	0.13	0.03	0.02	0.00	0.01	0.01	0.00	0.00	0.00	0.01	0.00	0.00
Heart	1.16	0.07	0.05	0.02	0.02	0.00	0.01	0.00	0.01	0.00	0.00	0.00	0.00	0.00
Intestinal contents, large	0.01	0.01	0.11	0.09	0.03	0.00	0.01	0.01	0.00	0.00	0.00	0.00	0.00	0.00
Intestinal contents, small	1.11	0.29	0.06	0.05	0.01	0.00	0.00	0.00	0.00	0.00	0.00	0.00	0.00	0.00
Intestine, large	1.52	0.08	0.65	0.11	0.16	0.09	0.03	0.02	0.02	0.00	0.01	0.00	0.00	0.00
Intestine, small	8.40	0.22	1.12	1.22	0.08	0.00	0.03	0.01	0.02	0.00	0.00	0.00	0.00	0.00
Kidneys	6.14	1.17	0.51	0.31	0.06	0.00	0.03	0.01	0.03	0.00	0.01	0.00	0.01	0.00
Liver	2.19	0.40	0.53	0.15	0.24	0.01	0.14	0.02	0.11	0.01	0.05	0.00	0.03	0.00
Lungs	1.57	0.12	0.10	0.03	0.03	0.00	0.02	0.00	0.01	0.00	0.01	0.00	0.00	0.00
Plasma	1.77	0.13	0.09	0.04	0.03	0.00	0.02	0.00	0.01	0.00	0.00	0.00	0.00	0.00
Skeletal muscle (pectoral)	1.50	0.21	0.05	0.02	0.00	0.00	0.00	0.00	0.00	0.00	0.00	0.00	0.00	0.00
Skeletal muscle (thigh)	1.44	0.28	0.07	0.03	0.00	0.00	0.00	0.00	0.00	0.00	0.00	0.00	0.00	0.00
Skin, nonpigmented	1.30	0.19	0.10	0.05	0.04	0.01	0.02	0.02	0.01	0.01	0.00	0.00	0.00	0.00
Skin, pigmented	1.34	0.25	0.09	0.02	0.01	0.01	0.00	0.00	0.00	0.00	0.00	0.00	0.00	0.00
Spleen	1.24	0.13	0.30	0.39	0.04	0.01	0.02	0.00	0.01	0.00	0.01	0.00	0.00	0.00
Stomach	5.54	1.51	0.20	0.11	0.04	0.00	0.02	0.00	0.01	0.00	0.00	0.00	0.00	0.00
Stomach contents	1.06	0.09	0.01	0.01	0.00	0.00	0.00	0.00	0.00	0.00	0.00	0.00	0.00	0.00
Testes	1.05	0.11	0.26	0.05	0.03	0.00	0.01	0.00	0.01	0.01	0.00	0.00	0.00	0.00
Thyroid	1.90	0.72	0.20	0.12	0.00	0.00	0.00	0.00	0.00	0.00	0.00	0.00	0.00	0.00
Urinary bladder	78.10	52.80	13.50	16.50	0.03	0.00	0.03	0.02	0.02	0.01	0.00	0.00	0.00	0.00

[a] μg-Eq of stavudine/g.

TABLE 2

Mean tissue/plasma ratios of stavudine-equivalent concentrations of radioactivity in rats after a single oral (5 mg/kg) administration of [1′-^{14}C]stavudine[a]

Matrix	Tissue/Plasma Concentration Ratios									
	Mean	S.D.	Mean	S.D.	Mean	S.D.	Mean	S.D.	Mean	S.D.
	1 h		*4 h*		*12 h*		*24 h*		*48 h*	
Adrenal glands	0.88	0.36	9.93	15.36	1.79	0.40	1.73	0.23	1.65	0.20
Blood	0.93	0.01	1.08	0.06	1.46	0.09	1.31	0.63	0.58	1.00
Bone (femur)	0.23	0.04	0.77	0.72	0.00	0.00	0.00	0.00	0.00	0.00
Bone marrow (femur)	0.99	0.03	1.67	1.11	1.44	1.26	0.00	0.00	0.00	0.00
Brain	0.16	0.02	1.00	0.15	0.49	0.08	0.36	0.09	0.28	0.24
Cecum	0.58	0.01	7.36	4.24	3.70	1.52	1.41	0.05	0.89	0.13
Eyes	0.63	0.12	1.40	0.16	0.70	0.09	0.24	0.27	0.10	0.18
Heart	0.66	0.02	0.58	0.01	0.50	0.07	0.49	0.10	0.54	0.29
Intestine, large	0.86	0.10	7.51	2.92	4.72	2.74	1.52	0.52	1.22	0.25
Intestine, small	4.76	0.46	14.43	17.31	2.49	0.19	1.28	0.12	1.20	0.11
Kidneys	3.45	0.44	6.01	4.73	1.80	0.07	1.52	0.12	1.85	0.28
Liver	1.23	0.14	6.12	2.78	7.20	0.43	6.98	0.37	7.83	0.07
Lungs	0.88	0.03	1.06	0.31	0.90	0.02	0.76	0.26	0.97	0.06
Skeletal muscle (pectoral)	0.85	0.06	0.54	0.04	0.00	0.00	0.00	0.00	0.00	0.00
Skeletal muscle (thigh)	0.81	0.11	0.79	0.44	0.00	0.00	0.00	0.00	0.00	0.00
Skin, nonpigmented	0.73	0.05	1.01	0.28	1.10	0.40	0.88	1.01	0.87	0.75
Skin, pigmented	0.76	0.09	0.96	0.30	0.15	0.25	0.00	0.00	0.00	0.00
Spleen	0.70	0.06	3.90	5.44	1.12	0.21	0.90	0.11	0.82	0.15
Stomach	3.13	0.77	2.29	1.61	1.14	0.07	0.90	0.07	0.82	0.07
Testes	0.59	0.02	2.87	0.48	0.95	0.07	0.64	0.12	0.39	0.34
Thyroid	1.08	0.44	2.25	1.79	0.00	0.00	0.00	0.00	0.00	0.00
Urinary bladder	44.68	30.57	181.00	225.53	0.83	0.03	1.29	0.69	1.07	0.92

[a] The data are presented only through 48 h because that was the last sampling time for which all the plasma concentrations were above the limit of quantitation.

sampling time for which all the plasma concentrations were above the limit of quantitation. The tissues with the highest maximal mean tissue/plasma concentration ratios were urinary bladder (181.00 at 4 h), followed by several intestinal tract tissues, adrenal glands, liver, and kidneys, with tissue/plasma values ranging from approximately 6 to 14. Heart, bone, skeletal muscle, and pigmented skin had mean ratios of <1 at all the sampling times. The lowest maximal mean ratios were for heart (0.66) and bone (0.77).

The mean maximal concentration of radioactivity (0.0833 μg-Eq/g) in expired air traps was observed at the first sampling time (0–6 h) after dosing. Mean concentrations at 6 to 12 h and 12 to 24 h were 0.0249 and 0.00330 μg-Eq/g, respectively. No radioactivity was trapped in expired air from 24 to 48 h postdose. A mean total of 0.94% of dosed radioactivity was recovered in expired air traps during the first 6 h after dosing. An additional mean total of 0.34% was recovered through 24 h postdose for an overall total of 1.28%.

Pharmacokinetics of Stavudine and Radioactivity in Humans. The plasma concentration versus time profiles for total radioactivity and unchanged stavudine in humans after a single oral administration of 80 mg of [1′-^{14}C]stavudine to six healthy male subjects are shown in Fig. 1. The pharmacokinetic parameters of stavudine and total radioactivity are summarized in Table 3. After oral administration of [1′-^{14}C]stavudine, peak plasma concentrations (T_{max}) of both stavudine and total radioactivity were achieved at 0.5 h, indicating rapid oral absorption. After the completion of absorption phase, concentrations of stavudine and total radioactivity decreased rapidly from plasma with no quantifiable amount detected after 24 and 8 h postdose, respectively, suggesting fast elimination. The rapid absorption and elimination of total radioactivity were also observed in rats where T_{max} for plasma was achieved at 1 h and T_{last} was achieved at 48 h postdose. The AUC(INF) value of 3363 ng·h/ml for stavudine was 61% of AUC(INF) value of radioactivity (5524 ng-Eq·h/ml), indicating a small but appreciable fraction of the circulating radioactivity was from metabolites. Approximately 67% of the administered stavudine dose was excreted as unchanged drug in urine. The average renal clearance of stavudine was 272 ml/min, and the mean oral clearance was 400 ml/min (Table 3).

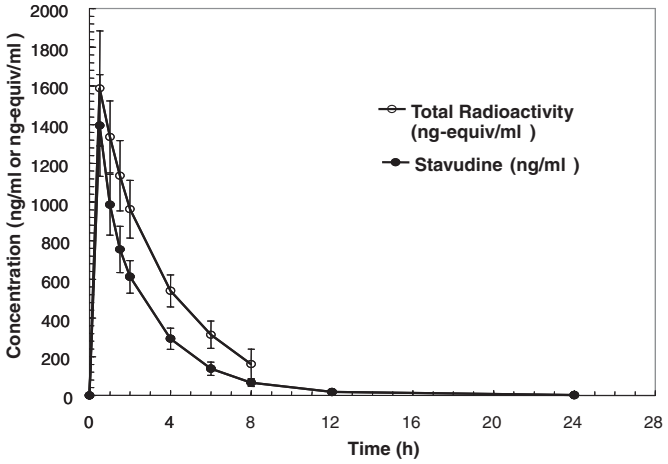

FIG. 1. Plasma concentration versus time profiles for total radioactivity and unchanged stavudine in humans after a single oral administration of 80 mg of [1′-^{14}C]stavudine to six healthy male subjects. Plasma stavudine was measured by HPLC/MS/MS analysis (LLOQ, 0.500 ng/ml). The total radioactivity, expressed as ng-Eq to stavudine, was measured by LSC and corresponds to stavudine and its metabolites (LLOQ, 120 ng/ml).

Recovery of Radioactivity in Humans. Greater than 70% of the radioactive dose was excreted in urine within 6 h (data not shown), and approximately 95% was recovered in the urine by 168 h (Table 3). Urinary excretion of administered dose was the predominant route of elimination in humans. Fecal excretion was limited, accounting for only 3% of the dose. The recovery of radioactivity was complete with 98% recovered in urine and feces combined.

Biotransformation Profiles in Human Plasma, Urine, and Feces. The biotransformation profiles of 1-h pooled plasma, 0- to 168-h pooled urine, and 0- to 168-h pooled feces are shown in Fig. 2. The relative distribution of radioactivity among various metabolite peaks in the radiochromatographic profiles of 1-h pooled plasma and 0- to

TABLE 3

Pharmacokinetic parameters of stavudine and total radioactivity in plasma after oral administration of [1′-^{14}C]stavudine to six healthy male subjects

Pharmacokinetic Parameter	Stavudine	Total Radioactivity
C_{max} (ng/ml or ng-Eq/ml), mean (CV%)	1372.9 (19.0)	1593.2 (17.0)
AUC(INF) (ng·h/ml or ng-Eq·h/ml), mean (CV%)	3362.9 (15.0)	5524.3 (19.0)
T_{max} (h), median (min, max)	0.5 (0.5, 0.5)	0.5 (0.5, 1.0)
T-half (h), mean (S.D.)	2.3 (0.5)	2.4 (0.6)
CLR (ml/min), mean (S.D.)	272.5 (80.3)	258.8 (54.1)
CLT/F (ml/min), mean (S.D.)	400.4 (61.3)	245.3 (49.2)
%UR, mean (S.D.)	67.2 (14.9)	95.1 (11.0)
%FE, mean (S.D.)	N.A.	2.7 (4.2)
%Total, mean (S.D.)[a]	N.A.	97.8 (10.3)

N.A., not applicable.
[a] %Total, percent of total administered dose recovered in urine and feces.

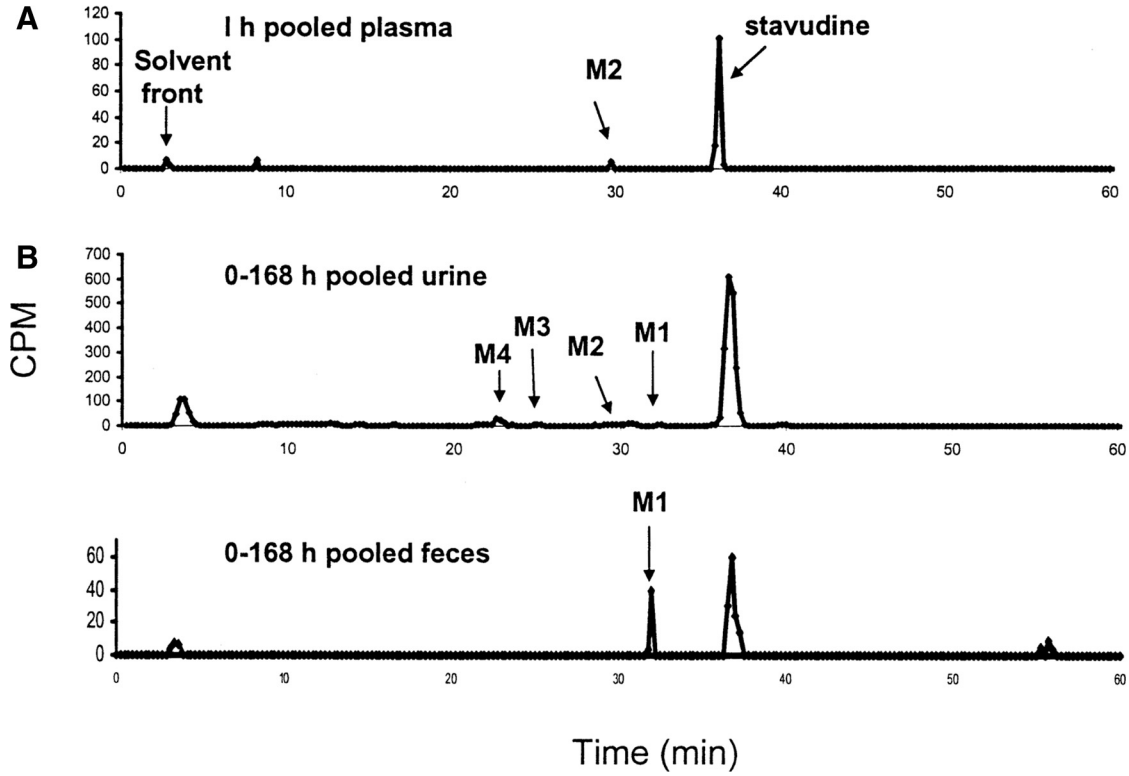

FIG. 2. Biotransformation profiles of 1-h pooled plasma (A), 0- to 168-h pooled urine, and 0- to 168-h pooled feces after single oral administration of 80 mg of [1′-^{14}C]stavudine to six healthy male subjects (B). A, the biotransformation profiles of 2-, 4-, and 6-h pooled plasma samples (data not shown) were qualitatively similar to the 1-h plasma profile. Only stavudine and metabolite M2 were observed in 1-, 2-, 4-, and 6-h pooled plasma. B, a small amount of radioactivity eluted with the solvent front in plasma, urine, and feces. Further chromatographic separation of the radioactivity in this region revealed at least five components in similar quantity (data not shown). Of the five components, only metabolite M5 was identified.

168-h pooled urine and feces is shown in Table 4. The peak for [1′-^{14}C]stavudine was identified based on its MS/MS fragmentation and comparison of its chromatographic retention time with a reference standard. The metabolite peaks were designated as M1 to M4 according to their relative HPLC retention times.

Unchanged stavudine accounted for 84.8% of radioactivity in 1-h pooled plasma (Table 4). It was also the most prominent peak in the biotransformation profiles of 2-, 4-, and 6-h pooled plasma samples (data not shown). Metabolites constituted minor components of the circulating radioactivity. Metabolite M2 accounted for 3.8% of the radioactivity in pooled 1-h plasma sample.

Unchanged stavudine was the major drug-related component in 0- to 168-h pooled urine, accounting for 73.7% of the radioactivity (67.2% of dose, Table 4). Metabolites M1 through M4 were detected as minor components, each accounting for <3.2% of the dose. Radioactivity eluting with the solvent front accounted for 13.1% of the administered radioactive dose. The radioactive peak at the solvent front, on isolation and separation by normal-phase HPLC, comprised five distinct peaks in similar radioactivity (data not shown). Of the five peaks, only one peak, metabolite M5, was identified. The identities of the other four peaks remain unknown.

Unchanged stavudine was also the major drug-related component in feces. It accounted for 62.0% (1.86% of dose) of the radioactivity. The other metabolite associated with feces was M1, accounting for 20.8% (0.62% of dose) of the radioactivity.

LC/MS/MS and NMR Characterization of the Metabolites. The structures of the metabolites were proposed based on their LC/MS/MS characterization. A summary of the mass spectral fragmentation of [1′-^{14}C]stavudine and its metabolites is compiled in Table 5. The protonated molecular ion of stavudine was observed at *m/z* 225. In its product ion spectrum, the ions at *m/z* 208 and 207 were consistent with losses of ·OH and H_2O, respectively, and the ion at *m/z* 165 was consistent with loss of

TABLE 4

Relative distribution of radioactivity (%) among various peaks in the radiochromatographic profiles of pooled 1-h plasma, 0- to 168-h urine, and 0- to 168-h feces after oral administration of [1′-^{14}C]stavudine to six healthy male subjects

Metabolite[a]	Retention Time	Percent Distribution in Pooled Samples[b]		
		1-h Plasma	0–168-h Urine	0–168-h Feces
			% of dose	*% of dose*
Stavudine	36.5	84.8	73.7 (67.2[c])	62.0 (1.9)
M1	32.1	N.D.	1.4 (1.3)	20.8 (0.6)
M2	29.8	3.8	0.3 (0.3)	N.D.
M3	25.0	N.D.	1.4 (1.3)	N.D.
M4	22.8	N.D.	3.3 (3.1)	N.D.
Solvent front[d] (containing M5)	2–3	6.9	13.8 (13.1)	8.8 (0.3)
Others[e]		4.5	6.1 (5.8)	8.4 (0.2)

N.D., not detected.

[a] Structures of metabolites are shown in Scheme 1.

[b] The relative percentage distribution of radioactivity represents the percentage of radioactivity in each peak compared with the total radioactivity recovered from the HPLC column eluant after background subtraction. The percentage of dose for metabolites was calculated from the relative percentage distribution of radioactivity and the average percentage of the radioactive dose excreted in the urine or feces.

[c] A validated LC/MS/MS assay was used for the determination of the concentration of stavudine in human urine. The percentage of dose for stavudine in urine was calculated from the amount of stavudine in urine and dose administered.

[d] These values represent the total radioactivity eluted with solvent front. M5 eluted with the solvent front in plasma, urine, and feces. Further chromatographic separation of the radioactivity in solvent front from the 0- to 168-h pooled urine samples revealed at least five components in similar radioactivity (data not shown). Of the five components, only metabolite M5 was identified. The structures of other four components were not identified.

[e] Remaining radioactivity distributed in small amounts in various fractions throughout the radiochromatogram.

TABLE 5

MS/MS fragmentation of [1′-^{14}C]stavudine and its metabolites detected in humans

Metabolites[a]	Positive Electrospray Ionization
Stavudine	MS, 225 MH^+; MS^2 on 225, 208 (MH^+-OH), 207 (MH^+-H_2O), 165 (MH^+-$HOCH_2CHO$), 127 (thymine moiety)
M1	MS, 241 MH^+; MS^2 on 241, 224 (MH^+- OH), 127 (thymine + H^+)
M2	MS, 417 MH^+; MS^2 on 417, 399 (MH^+-H_2O), 241 (MH^+-glucuronide); MS^3 on 241, 224 (MH^+-glucuronide and -OH), 223 (MH^+-glucuronide, and -H_2O), 213 (MH^+-glucuronide and -CO), 195 (MH^+-glucuronide, -CO, and -H_2O)
M3	MS, 401 MH^+; MS^2 on 401, 225 (MH^+-glucuronide); MS^3 on 225, 207 (MH^+-glucuronide, and -H_2O)
M4[b]	MS, 278 MH^+; MS^2 on 278, 260 (MH^+-H_2O); 218 (MH^+-H_2O and -CH_2CO); 164 (NAC + H^+); 162 (MH^+-ribose moiety)
M5	MS, 259 MH^+; MS^2 on 259, 242 (MH^+-OH), 241 (MH^+-H_2O); 127 (thymine moiety)

[a] Structures of metabolites are shown in Scheme 1.

[b] Accurate mass measurement was done for metabolite M4 and it fragments. MS, 278.06943 MH^+; MS^2 on 278.06943, 260.05840 (MH^+-H_2O), 218.04780 (MH^+-H_2O and -CH_2CO), 164.03731 (NAC + H^+), 162.02167 (MH^+-ribose moiety).

a $HOCH_2CHO$. The elimination of the ribose moiety by cleavage of the glycosidic bond yielded the protonated thymine at *m/z* 127. Similar fragmentation was observed for a stavudine reference standard.

Metabolite M1 was determined to be an oxidation product of stavudine. The protonated molecular ion of M1 was observed at *m/z* 241, which is 16 Da higher than that of the parent. The base peak in the product ion spectrum was observed at *m/z* 224, consistent with loss of a hydroxyl radical (·OH). The presence of an ion at *m/z* 127, previously assigned as protonated thymine, suggested that the oxidation had occurred on the ribose moiety.

Metabolite M2 was identified as a glucuronide of the oxidized product of stavudine. The protonated molecular ion of M2 was observed at *m/z* 417. Fragmentation of the *m/z* 417 precursor yielded an ion at *m/z* 241, attributable to a neutral loss of 176 Da from the molecular ion, indicating that M2 is a glucuronide conjugate. The base peak in the product ion spectrum, *m/z* 399, was consistent with H_2O loss from the protonated molecular ion. Based on the observation of an ion at *m/z* 241, also seen for protonated molecular ion of M1, M2 was assigned as a glucuronide of oxidized stavudine. The MS^3 spectrum of M2 (*m/z* 417→*m/z* 241→) contained a major fragment at *m/z* 223 and a minor fragment at *m/z* 224, consistent with losses of H_2O and ·OH, respectively. The ions at *m/z* 213 and 195 could potentially arise from sequential losses of CO and H_2O molecules from *m/z* 241.

Metabolite M3 was identified as a glucuronide conjugate of the parent. The protonated molecular ion of M3 was observed at *m/z* 401. The base peak in the product ion spectrum, *m/z* 225, was generated by a neutral loss of 176 Da, indicating that M3 is a glucuronide conjugate. The MS^3 spectrum of M3 (*m/z* 401→*m/z* 225→) contained product ions consistent with stavudine, supporting the assignment of M3 as a glucuronide conjugate of stavudine, most likely linked through the terminal OH group on the ribose moiety.

Metabolite M4 showed a protonated molecular ion at *m/z* 278. The product ion spectrum obtained from *m/z* 278 gave rise to two abundant ions at *m/z* 164 and 162, consistent with an NAC molecule. The tentative assignment of M4 was an NAC conjugate of the ribose after a glycosidic cleavage. To confirm the structure, metabolite M4 was isolated from pooled 0- to 24-h urine of subject 5 and characterized by accurate mass, MS/MS, and NMR analyses. The elemental compositions determined for *m/z* 278 and its product ions agreed with the proposed structure. The 1D-^{1}HNMR spectrum of M4 with peak assignment is shown in Fig. 3A. The TOCSY spectra are shown in Fig. 3, B and C. A proton spin system consistent with the presence of a cysteine moiety was observed in the TOCSY spectrum (highlighted in the rectangle in Fig. 3B). The TOCSY spectrum of the aliphatic region showed a continuous four-bond proton spin system, which excluded the possibility of existence of double bond between either carbons 2 to 3 or carbons 3 to 4 in the ribose ring (highlighted in the rectangle in Fig. 3C and circled on the structure in Fig. 3). The NMR analysis, together with information provided by accurate mass analysis, confirmed the proposed structure for metabolite M4.

Metabolite M5 was a bis-oxidation product of stavudine. The protonated molecular ion for M5 was observed at *m/z* 259. The

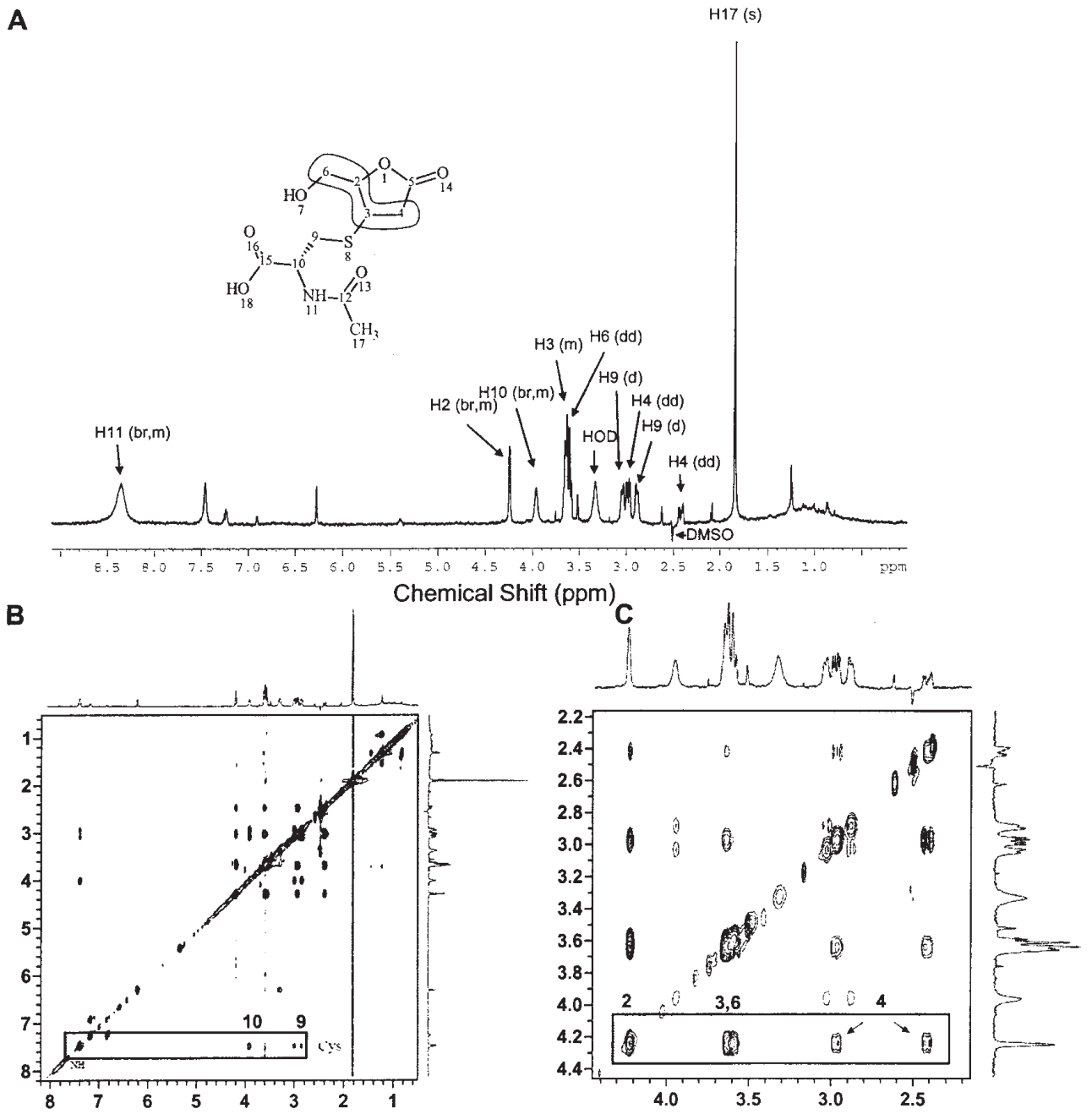

FIG. 3. One-dimensional proton spectrum (A) and ^{1}H-^{1}H TOCSY of metabolite M4 (B and C). C, shows the enlarged ^{1}H-^{1}H TOCSY of the aliphatic region. Abbreviations used on the resonances are as follows: d, doublet; dd, doublet of doublet; s, singlet; m, multiple; br, broad peak.

product ion spectrum exhibited fragmentation consistent with a bis-oxidation product of stavudine, including ions at *m/z* 242, 241, and 127.

Generating [1′-^{14}C]2′,3′-Didehydrodideoxyribose. Acidic hydrolysis of [1′-^{14}C]stavudine was conducted to obtain [1′-^{14}C]2′,3′-didehydrodideoxyribose (Shapiro and Danzig, 1972). With time, the disappearance of [1′-^{14}C]stavudine from the reaction solution was accompanied by the appearance of a radioactivity peak at retention time of 17 min. LC/MS/MS analysis of the emerging peak was consistent with its assignment as [1′-^{14}C]2′,3′-didehydrodideoxyribose (data not shown). Its protonated molecular ion was observed at *m/z* 117 in the mass spectrum. Product ions at *m/z* 99 and 89 were consistent with losses of H_2O and CO, respectively. Thymine, the byproduct of [1′-^{14}C]stavudine hydrolysis, was also observed in the reaction mixture at retention time of 14.8 min by LC/MS detection. Less than 30% of the [1′-^{14}C]stavudine substrate remained after 2-h reaction.

Formation of Metabolite M4 in Human Liver Microsomes. Metabolite M4 was regenerated in vitro when human liver microsomes were incubated with [1′-^{14}C]2′,3′-didehydrodideoxyribose in the presence of NAC. The incubation substrates, generated above, were a mixture of [1′-^{14}C]2′,3′-didehydrodideoxyribose, thymine, and [1′-^{14}C]stavudine in a ratio of 7:7:3 (data not shown). The MS/MS fragmentation and HPLC retention time of metabolite M4 purified from human urine were used as references for detection of metabolite M4 in human liver microsomes. The biotransformation profiles of the mixture of [1′-^{14}C]2′,3′-didehydrodideoxyribose, thymine, and [1′-^{14}C]stavudine with human liver microsomes in the presence or absence of NAC are shown in Fig. 4,

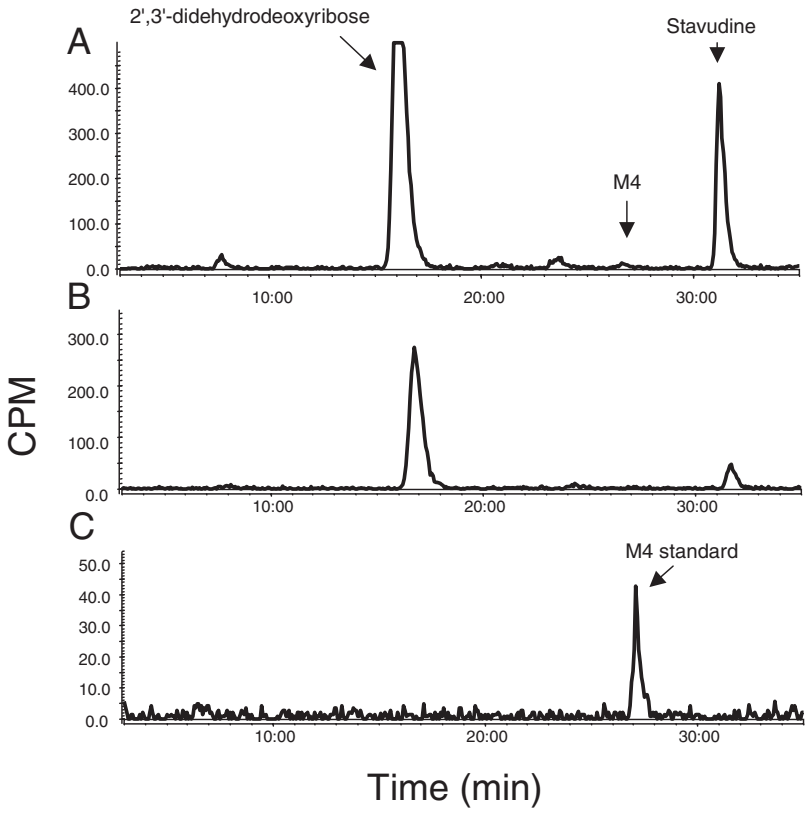

FIG. 4. Biotransformation profiles of a mixture of 2′,3′-didehydrodideoxyribose, thymine, and stavudine (7:7:3) in human liver microsomes in the presence (A) or absence (B) of NAC. C, shows the radiochromatogram of metabolite M4 standard isolated from human urine. Note: thymine was not detected by radioactivity detection because it was not radiolabeled.

A and B, respectively. Figure 4C presents the radiochromatogram of M4 that was isolated from urine. The turnover of [1′-^{14}C]2′,3′-didehydrodideoxyribose was very low in human liver microsomes. No major metabolites were observed. Metabolite M4 was detected as a minor peak at retention time of 27 min in the radiochromatogram. Two additional minor radioactivity peaks were observed but remain unidentified in the sample derived from incubations with human liver microsomes fortified with NAC. Metabolite M4 was not generated when the incubation was not fortified with NAC (Fig. 4B). No metabolites were observed when human liver microsomes were incubated with either [1′-^{14}C]stavudine or thymine in the presence or absence of NAC.

Formation of GSH Conjugates in Human Liver Microsomes. Detection of GSH conjugates was performed by looking for the characteristic fragmentations for a GSH adduct in the product ion spectrum. Two GSH conjugates were detected in the microsomal incubations of [1′-^{14}C]2′,3′-didehydrodideoxyribose, thymine, and [1′-^{14}C]stavudine in the presence of NADPH and GSH. Of the two detected GSH conjugates, one, assigned as 3′-GS-ribose, had a retention time of 12.2 min, exhibiting a protonated molecular ion at *m/z* 440. The base peak in the product ion spectrum of *m/z* 440 was observed at *m/z* 311, consistent with neutral loss of pyroglutamate (129 Da). Other ions included *m/z* 423, loss of NH3 (17 Da); *m/z* 365, loss of glycine (75 Da); and *m/z* 179, protonated cysteinylglycine (Fig. 5). The other GSH conjugate, assigned as 1′-keto-2′,3′-dideoxy-3′-GS-ribose, was observed at retention time of 18.1 min by LC/MS/MS detection. Its protonated molecular ion was observed at *m/z* 422. Ions characteristic of GSH adducts, including *m/z* 293 (loss of 129 Da) and *m/z* 422 (loss of 75 Da), were observed in its product ion spectrum. Both GSH conjugates were minor metabolites and only detectable by LC/MS/MS analysis. No radioactivity peaks representing these metabolites were observed. No metabolites were observed when human liver microsomes were incubated with either [1′-^{14}C]stavudine or thymine alone in the presence or absence of GSH.

Discussion

The study with a radiolabeled version of a new chemical entity in humans is a key study conducted to understand the role of metabolic pathways or direct excretion in the elimination of drug-related material. One of the key considerations before initiating this study is the placement of the radiolabel. If the label is incorporated in a metabolically labile moiety of the molecule, there is a chance it may be liberated through metabolism. If the labeled labile moiety is similar to an endogenous compound, there may be incorporation into cellular components or loss as $^{14}CO_2$ via endogenous catabolism. These events could lead to poor recovery of radioactivity and to safety concerns as there could be extended exposure to radioactivity. Therefore, labeling the appropriate part of the molecule becomes critical to ensure good recovery of the dose when dosed to humans. For stavudine, studies with thymine-labeled material in animals had shown that there could be significant loss through release of thymine and its metabolism through endogenous pathways. Therefore, for the human ADME study, the ^{14}C-label was incorporated on the ribose ring. To confirm that this was a metabolically stable position, a tissue distribution study was conducted in rats with the ^{14}C-ribose-labeled stavudine ([1′-^{14}C]stavudine). Only ~1.2% of the dose was recovered in expired air as $^{14}CO_2$ in this study compared with a loss of 14% of the dose as $^{14}CO_2$ with thymine-labeled stavudine reported in a previous study in rats, suggesting a nonsignificant fraction of the dose may be shunted into an endogenous biochemical pathway with ^{14}C-ribose-labeled stavudine. Moreover, there was no significant accumulation in the tissues, particularly in the eyes and the skin, suggesting that the [1′-^{14}C]stavudine would be appropriate for dosing to humans. This was confirmed when 98% of the dose was recovered in the human ADME study.

This study showed that [1′-^{14}C]stavudine was completely absorbed and eliminated with urinary excretion of unchanged drug as the predom-

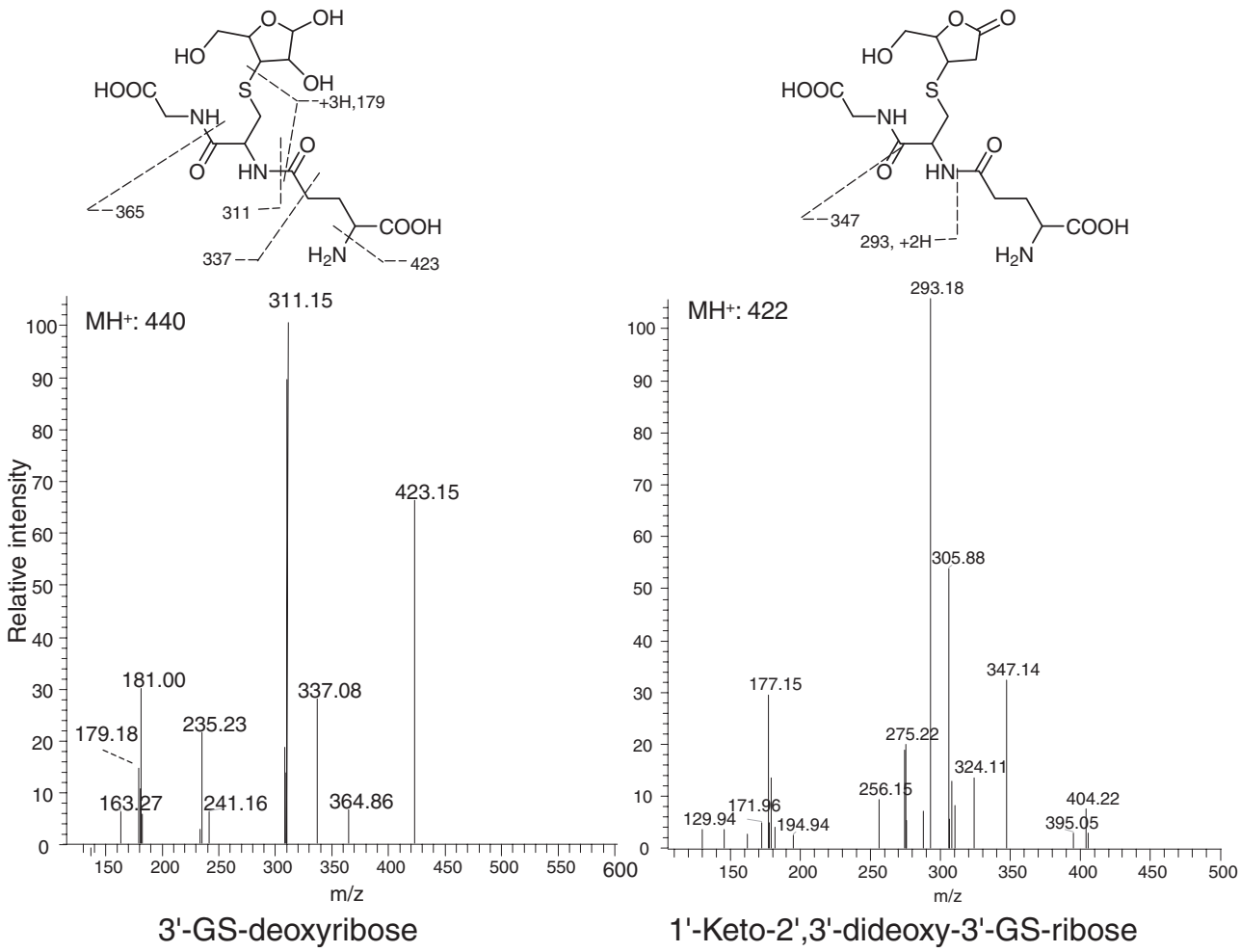

FIG. 5. MS/MS spectra and fragmentation of 3′-GS-deoxyribose and 1′-keto-2′,3′-dideoxy-3′-GS-ribose, which were detected in the microsomal incubations of [1′-^{14}C]2′,3′-didehydrodideoxyribose in the presence of NADPH and GSH.

inant route of elimination after oral dosing to humans. The route of elimination in humans is in concurrence with the findings in mice, rats, and monkeys (Russell et al., 1990; Cretton et al., 1993; Kaul and Dandekar, 1993; Kaul et al., 1999). The extent of absorption and oral bioavailability of stavudine in humans was at least 95 and 67%, respectively, based on urinary recovery values of TRA and stavudine. Consistent with the observation in animals, unchanged stavudine was the major drug-related component in plasma, urine, and feces in humans. It is obvious that metabolism played a limited role in the elimination of stavudine. Five minor metabolites of stavudine were identified in the study, including mono- and bis-oxidation products (M1 and M5), glucuronide of stavudine (M3) and its oxidized metabolite (M2), and an NAC conjugate of the ribose after glycosidic cleavage (M4). Formation of M4 requires glycosidic cleavage of [1′-^{14}C]stavudine, and by inference thymine is released in this reaction. No quantitative estimate for thymine and its breakdown products are provided in this study because the ^{14}C-label was on the ribose ring. However, it is expected that the thymine formed would undergo the normal biochemical pathways of metabolism known for pyrimidine nucleosides (Moran et al., 1994). The endogenous thymine catabolism involves reduction of thymine to dihydrothymine. Hydrolysis of the latter gives rise to β-ureidoisobutyric acid, which is further hydrolyzed to β-aminoisobutyric acid, CO_2, and NH_3. The β-aminoisobutyric acid can be partly excreted intact in the urine, can be further metabolized to other compounds such as methylmalonate, an intermediate in the metabolism of propionic acid, or can be subjected to further oxidation and ultimately to CO_2 and H_2O (Niemann and Berech, 1981; Griffith, 1986). The proposed biotransformation pathways for [1′-^{14}C]stavudine are shown in Scheme 1.

It is well known that stavudine is metabolized in cells to the mono-, di-, and triphosphate nucleotides. Furthermore, the intracellular concentration of stavudine triphosphate has been correlated with its antiviral activity. The presence of extracellular stavudine mono-, di-, and triphosphate has not been established, nor did we detect any of the three phosphorylated species of stavudine in this study. One possible explanation is that the phosphorylated species of stavudine are trapped in the cells because of their poor permeability resulting from their good hydrophilicity and lack of transporter-mediated transport across the cell membrane. This is true for a number of nucleoside drugs where their cellular uptake and formation of the mono-, di-, and triphosphate nucleotides are necessary for activity. In those cases, these metabolites also are not recovered extracellularly for the reasons mentioned above (Balzarini, 1994).

The results of this study indicate the types of clinical studies that may be needed in the development of stavudine as part of assessment of its safety and effectiveness. These indications can be applied to a new chemical entity with a similar ADME profile. Because of the limited contribution of hepatic clearance to its overall elimination, the impact on pharmacokinetics of stavudine is expected to be low when coadministered with drugs that are inducers or inhibitors of cytochromes P450 or other metabolic enzymes. For the same reason,

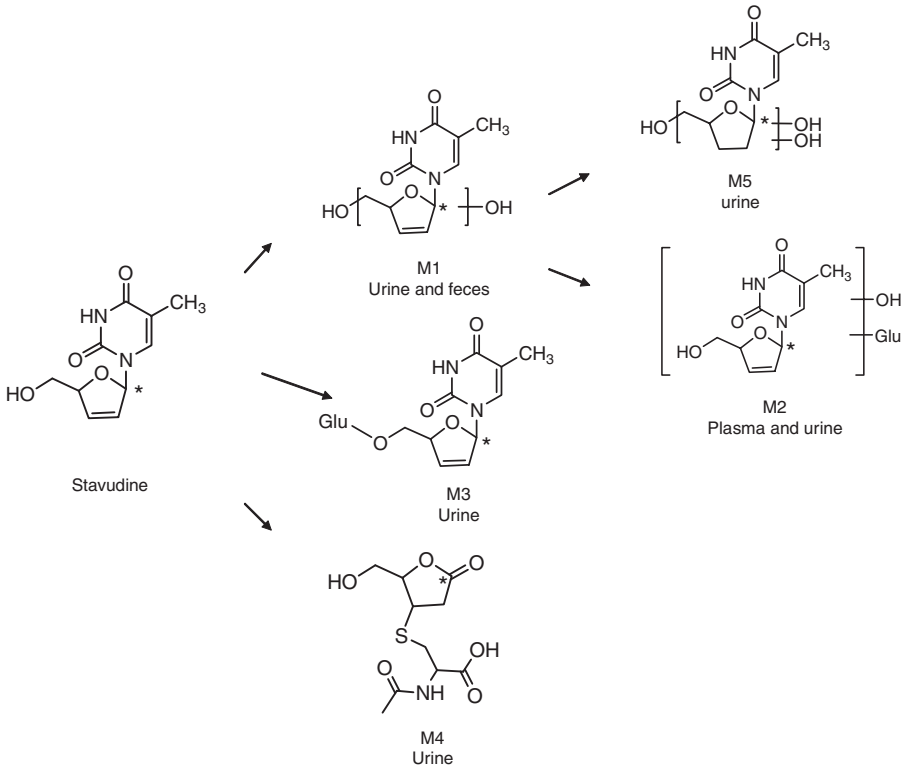

SCHEME 1. Proposed biotransformation pathways for [1′-^{14}C]stavudine in humans. ∗, denotes the location of the ^{14}C-label. Note: because [1′-^{14}C]stavudine undergoes glycosidic cleavage, by inference, thymine should also be a metabolite of stavudine. However, no quantitative estimate for thymine and its breakdown products are provided in this study because the ^{14}C-label was on the ribose ring. However, it is expected that the thymine formed from stavudine in humans would undergo metabolism via the normal biochemical pathways known for pyrimidine nucleosides.

stavudine pharmacokinetic parameters in subjects with hepatic impairment are not expected to be altered; thus, dose adjustment will not be necessary. Indeed, clinical study showed that stavudine pharmacokinetics in subjects with hepatic impairment was similar to those in age- and gender-matched control subjects and was not substantially different from those previously observed in HIV-infected patients (Schaad et al., 1997). On the other hand, patients with renal impairment may have altered pharmacokinetics of stavudine because of the significant contribution of renal excretion to its overall elimination. This suggestion has been confirmed by two clinical studies where the oral clearance of stavudine decreased as creatinine clearance decreased. Therefore, stavudine dosage is recommended to be modified in patients with reduced creatinine clearance and in patients receiving maintenance hemodialysis (Grasela et al., 2000). Furthermore, the values of the mean terminal elimination half-life (2.3 h), mean renal clearance (272.5 ml/min), mean oral clearance (400.4 ml/min), and mean percentage of administered dose excreted in urine (67.2) determined in this study are all consistent with the observations of the other clinical studies in healthy subjects (Schaad et al., 1997; Grasela et al., 2000).

Investigation into the formation of metabolite M4 showed that an epoxide intermediate was involved. The origin of metabolite M4

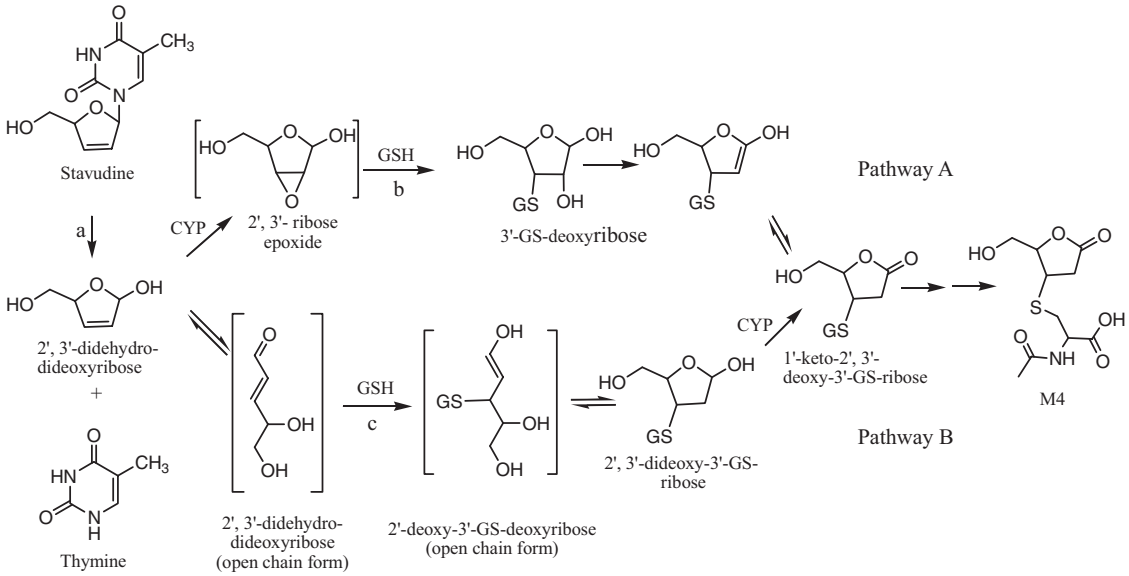

SCHEME 2. Two hypothetical metabolic pathways proposed for the formation of metabolite M4 in humans. A, *N*-Glycosidic bond cleavage. B, GSH epoxide addition. C, 1,4-Michael addition. Note: incubation of human liver microsomes with 2′,3′-didehydrodideoxyribose in the presence of GSH revealed intermediate 3′-GS-deoxyribose but not 2′,3′-dideoxy-3′-GS-ribose. This result lends support to pathway A over pathway B.

likely involves formation of a GSH conjugate in the liver and subsequent conversion to an NAC conjugate via the mercapturic acid formation pathway (Moran et al., 1994). The fact that direct conjugation of stavudine with GSH or NAC was not observed in either humans or human liver microsomes suggested that *N*-glycosidic bond cleavage is a prerequisite for formation of metabolite M4. Thus, it is postulated that the formation of the GSH conjugate is through generation of an epoxide on the ribose ring after *N*-glycosidic bond cleavage. Two distinct pathways are thereby proposed after *N*-glycosidic bond cleavage. One proceeds by oxidation of the unsaturated bond between the 2′- and 3′ carbons of 2′,3′-didehydrodideoxyribose to form an epoxide intermediate, followed by addition of GSH (Scheme 2, pathway A). A second pathway could involve opening the ribose ring to generate an α,β-unsaturated ketone that undergoes 1,4-Michael addition reaction with GSH (Scheme 2, pathway B). Both epoxides and α,β-unsaturated ketones have been reported to be excellent substrates for GSH addition reaction (Blair, 2006). The *N*-glycosidic bonds of nucleoside analogs can be cleaved either enzymatically by nucleoside hydrolases or nonenzymatically under acidic conditions (Shapiro and Danzig, 1972). In this study, acid hydrolysis of the *N*-glycosidic bond of stavudine was used to form 2′,3′-didehydrodideoxyribose. Incubation of human liver microsomes with 2′,3′-didehydrodideoxyribose in the presence of GSH generated 3′-GS-deoxyribose and its subsequent product by loss of a water, 1′-keto-2′,3′-dideoxy-3′-GS-ribose. This suggests that 2′,3′-didehydrodideoxyribose must have undergone cytochrome P450-mediated oxidation leading to an epoxide intermediate 2′,3′-ribose epoxide. The absence of a 2′,3′-dideoxy-3′-GS-ribose product suggests that the addition of GSH to an α,β-unsaturated ketone intermediate was not occurring in these incubations. Therefore, the involvement of the 1,4-Michael addition in the pathway for formation of metabolite M4 is not concluded to be the primary pathway. Metabolite M4 was generated in vitro in incubation of 2′,3′-didehydrodideoxyribose and NAC with human liver microsomes. However, because no intermediates could be identified, it is not clear by which pathway 2′,3′-didehydrodideoxyribose interacts with NAC. Epoxides as electrophilic reactive intermediates are expected to be capable of formation of adducts with proteins, RNAs, or DNAs and thus may contribute to drug-related adverse effects (Blair, 2006). However, metabolite M4 accounted for only 3.1% of the administered dose of stavudine. Given that the clinical dose of stavudine is $<$100 mg, of which only a small percentage is converted to metabolite M4, it is unlikely that the epoxide-reactive intermediate would contribute to any stavudine-related toxicity.

In conclusion, absorption and elimination of [1′-^{14}C]stavudine were rapid and complete after oral dosing, with urinary excretion of the unchanged drug as the predominant route of elimination in humans. Stavudine was the only major drug-related component in plasma, and metabolism played a limited role in its elimination.

Acknowledgments. We thank Dr. Donghui Cui (Merck, West Point, PA) for helpful discussions.

References

Balzarini J (1994) Metabolism and mechanism of antiretroviral action of purine and pyrimidine derivatives. *Pharm World Sci* **16:**113–126.

Blair IA (2006) Endogenous glutathione adducts. *Curr Drug Metab* **7:**853–872.

Cretton EM, Zhou Z, Kidd LB, McClure HM, Kaul S, Hitchcock MJ, and Sommadossi JP (1993) In vitro and in vivo disposition and metabolism of 3′-deoxy-2′,3′-didehydrothymidine. *Antimicrob Agents Chemother* **37:**1816–1825.

Discordia RP (1996) Synthesis of [1′-^{14}C]stavudine (d4T). *J Labelled Comp Rad* **38:**614–623.

Grasela DM, Stoltz RR, Barry M, Bone M, Mangold B, O'Grady P, Raymond R, and Haworth SJ (2000) Pharmacokinetics of single-dose oral stavudine in subjects with renal impairment and in subjects requiring hemodialysis. *Antimicrob Agents Chemother* **44:**2149–2153.

Griffith OW (1986) Beta-amino acids: mammalian metabolism and utility as alpha-amino acid analogues. *Annu Rev Biochem* **55:**855–878.

Huang P, Farquhar D, and Plunkett W (1992) Selective action of 2′,3′-didehydro-2′,3′-dideoxythymidine triphasphate on human immunodeficiency virus reverse transcriptase and human DNA polymerases. *J Biol Chem* **267:**2817–2822.

Institute of Laboratory Animal Resources (1996) *Guide for the Care and Use of Laboratory Animals*, 7th ed. Institute of Laboratory Animal Resources, Commission on Life Sciences, National Research Council, Washington DC.

International Commission on Radiological Protection (2008) *Publication 103: Recommendations of the ICRP*, Elsevier, Philadelphia.

Kaul S and Dandekar KA (1993) Pharmacokinetics of the anti-human immunodeficiency virus nucleoside analog stavudine in cynomolgus monkeys. *Antimicrob Agents Chemother* **37:**1160–1162.

Kaul S, Dandekar KA, Schilling BE, and Barbhaiya RH (1999) Toxicokinetics of 2′,3′-didehydro-3′-deoxythymidine, stavudine (D4T). *Drug Metab Dispos* **27:**1–12.

Lea AP and Faulds D (1996) Stavudine: a review of its pharmacodynamic and pharmacokinetic properties and clinical potential in HIV infection. *Drugs* **51:**846–864.

Moran LA, Scrimgeour KG, Horton HR, and Rawn JD (1994) *Biochemistry*, pp 22.26–22.27, Neil Patterson, Englewood Cliffs, NJ.

Niemann MA and Berech J Jr (1981) Thymidine catabolism and the reutilization of its degradative products in Tetrahymena pyriformis. Metabolism of [2,6-14C2]thymidine and [2-14C]methylmalonic acid. *Biochim Biophys Acta* **652:**347–353.

Russell JW, Whiterock VJ, Marrero D, and Klunk LJ (1990) Disposition in animals of a new anti-HIV agent: 2′,3′-didehydro-3′-deoxythymidine. *Drug Metab Dispos* **18:**153–157.

Schaad HJ, Petty BG, Grasela DM, Christofalo B, Raymond R, and Stewart M (1997) Pharmacokinetics and safety of a single dose of stavudine (d4T) in patients with severe hepatic impairment. *Antimicrob Agents Chemother* **41:**2793–2796.

Shapiro R and Danzig M (1972) Acid hydrolysis of deoxycytidine and deoxyuridine derivatives. The general mechanism of deoxyribonucleoside hydrolysis. *Biochemistry* **11:**23–29.

Siegfried NL, Van Deventer PJ, Mahomed FA, and Rutherford GW (2006) Stavudine, lamivudine and nevirapine combination therapy for treatment of HIV infection and AIDS in adults. *Cochrane Database Syst Rev* **2:**CD004535.

Zhu M, Zhao W, Vazquez N, and Mitroka JG (2005) Analysis of low level radioactive metabolites in biological fluids using high-performance liquid chromatography with microplate scintillation counting: method validation and application. *J Pharm Biomed Anal* **39:**233–245.

Address correspondence to: Lian Zhou, Bristol Myers Squibb Co., P.O. Box 4000, Princeton, NJ 088543. E-mail: lian.zhou@bms.com